PHYSICAL REVIEW A VOLUME 21, NUMBER 4 APRIL 1980

X-ray line shift as a high-density diagnostic for laser-imploded plasmas

Stanley Skupsky
Laboratory for Laser Energetics, University of Rochester, 250 East River Road, Rochester, New York 14623
(Received 13 November 1979)

The frequency shift of x-ray spectral lines has been theoretically studied for possible application as a density diagnostic in high-compression laser-fusion experiments. Neon was found to have line-shift characteristics ideal for near-term experiments and could be used as a diagnostic seed material for the fuel. At densities above ~ 4 g/cm^3, the shift of neon Lyman α was found to be roughly proportional to density ($\Delta\hbar\omega \approx -2\times 10^{-24} n_e$ eV). The calculations were done by solving the Schrödinger equation for energy levels, in a self-consistent potential determined by the nonlinear Poisson equation for electrons and neighboring ions. The computer simulation of a possible laser-compression experiment was used to calculate the line spectrum that might be seen in the laboratory and to illustrate how the shift could be used to estimate density. Unfortunately, this diagnostic was found to be applicable only when the average charge of target materials was less than about 6; i.e., it is applicable to plastic microballoons but not to glass. When higher-Z material is present, then the amount of background radiation and line attenuation reduce neon Lyman α to the level of noise and preclude an accurate measure of the frequency shift. Alternatively, given other diagnostics for density, such experiments could be used to test the theory of line shifts and to examine the physics of ions in a high-density plasma.

I. INTRODUCTION

One of the near-term goals of laser-fusion experiments is to obtain and clearly diagnose compressed deuterium-tritium (DT) fuel densities in the region around 100 times the density of liquid hydrogen. Past experiments have relied heavily on spectral line broadening for measuring density.[1] Present and future experiments will continue to use line broadening as well as neutron diagnostics such as activation[2] and knock-ons.[3] A potential diagnostic that has not yet been considered is the frequency shift of spectral lines from high-Z ions added to the DT fuel. A frequency shift is expected, due to shielding of the nucleus by free electrons. The amount of shift will be determined by the mean distribution of electrons and neighboring ions. As an example, the neon Lyman-α line was calculated to shift about 10 eV at a density of 20 g/cm^3. Fluctuations around the mean will then result in line broadening. As shown below, the amount of shift should be sensitive to the high densities anticipated for laser-fusion experiments. These experiments will be able to test the theory of line shifts in a density region hitherto unattainable in the laboratory. If the results are favorable, then the line shift could be used in future experiments as a diagnostic for density in low-Z targets. If there are deviations from theory, then the experiments become a means for examining the physics of ions in a high-density plasma.

The possibility that free electrons can cause a shift of spectral lines has been discussed for over 15 years, and is often referred to as the plasma polarization shift.[4] Early theoretical models of the shift were not satisfactory, being based on linearized Debye-Hückel (DH) theory. The linearization is valid at large distances from the ion, but not close to the nucleus where the model was applied. It is not surprising that the model incorrectly predicted even the direction of the experimental line shift; the calculation predicted a red shift, whereas the experimental observation was a shift toward the blue. Other calculations assumed that the electrons were uniformly distributed.[5] This also incorrectly produced a red shift, as approximations in the model were not applicable to the low-density experiments. However, at much higher densities, this uniform-electron model does give qualitatively the same answers as a more detailed picture of the free electrons, which is discussed in Sec. II A. In that section, it is shown that the line shift for neon Lyman α should change from blue to red at an electron density of about 10^{24} cm^{-3} ($\rho \sim 4$ g/cm^3), and its magnitude should increase almost linearly with density, in agreement with results of the uniform-electron model. In this region the theory is most sound and this is just the region being explored in the near-term laser-fusion experiments. Such a transition from blue to red should occur also for lower-Z materials at lower densities (Sec. II C), but it still is above the range of past line-shift experiments and has not been seen. Below the transition density the line shift is so small that the theoretical results are questionable. However, above the transition density, the shift can grow sufficiently large that a clear-cut comparison between theory and experiment can be made.

Perhaps the most sophisticated calculations of

the line shift were made by Rozsnyai[6] in 1974. He calculated a self-consistent potential to determine the effect of electron shielding. The free electrons were treated statistically as in the Thomas-Fermi model, and the bound electrons were calculated according to the Hartree-Fock-Slater approach. The Coulomb potential of the ion was chosen to vanish on a sphere around the ion whose diameter was equal to the interion distance. This is the usual "ion-sphere" boundary condition of Thomas-Fermi theory and should be valid at high density when the ions become correlated. However, it is not justified at low density, since it does not yield the standard result given by the Debye-Hückel theory. Nevertheless, when this model was applied to the low-density experiments, it correctly gave the direction of the line shift (to the blue), though the magnitude was too large.

The approach here differs from that taken by Rozsnyai mainly in the choice of boundary conditions and in the region of temperature and density where the model was used. Since the model will be applied to a high-Z ion in a deuterium-tritium plasma, it would not be justified to neglect shielding of the nucleus by the DT ions. This effect is not included with ion-sphere boundary conditions. Thus, to treat the shielding of the nucleus, the Coulomb potential was extended to infinity using shielding given by *nonlinear* Debye-Hückel theory for both the ions and electrons. This is the same boundary condition used by Stewart and Pyatt[7] and by Cowen and Kirkwood.[8] It has the advantage of giving the correct boundary condition at both low and high density, and it interpolates smoothly between these extremes. At high density, the nonlinear Debye-Hückel model pushes neighboring ions of the ionic sphere and drags in enough free electrons to neutralize the ion. Then the potential is effectively zero at the boundary of the sphere, and it approximates the ion-sphere boundary conditions used by Rozsnyai and used in most Thomas-Fermi calculations. At low density, the usual Debye-Hückel shielding is recovered.

This model was applied to calculation of the neon Lyman-α frequency shift. Neon Lyman α appears to be the best candidate for near-term laser-fusion experiments designed for densities around 20 g/cm^3 (100 times liquid-DT density). The line emission is sufficiently intense at the temperatures of 500–1000 eV anticipated near peak density, and the shift should be about 10 eV which is easily detected and is above theoretical uncertainties in the model. Further, neon is relatively easy to handle for target fabrication. Radiation from lower-Z materials would be lost in the background. Lines from higher-Z ions require a temperature about $(Z/10)^2$ times higher and a density $(Z/10)^4$ times higher to produce the same fractional line shift as in neon. Scaling arguments in Sec. IIC show that the fractional change in the line frequency is given by

$$\Delta E/E_0 \approx 5\rho/Z^4 .$$

Unfortunately, the line shift cannot be used as a diagnostic for the general laser-fusion target. If there is much material present with average charge greater than about 6, then the amount of continuum radiation and line attentuation would reduce the neon Lyman α to the level of background noise. This essentially constrains the target to be a plastic microballoon; glass-shelled targets are already too high in Z.

The format of this paper is as follows. Details of the atomic model are discussed in Sec. II (and in the Appendix). Application of the model to neon Lyman α is discussed in Sec. III, where results are presented for the line-shift variation as a function of temperature and density. Section IV discusses the computer simulation of a possible laser implosion experiment and calculates the expected line profile from a neon impurity added to the DT fuel for diagnostic purposes. Included in the calculation is the frequency shift, line broadening, and the superposition of profiles resulting from line emission at different times and different densities during the implosion. The results show that for the time-integrated line profile, it would be difficult to extract information about peak density. However, if the line emission can be time resolved with an x-ray streak camera then the line shift should be observable and could become a density diagnostic in future laser compression experiments for low-Z targets. There should be no problem regarding a reference point for measuring the shift. Early line emission from low density produces a marker at the unshifted frequency.

II. FORMALISM

A. Self-consistent potential

To describe why a spectral line changes frequency with density, it is convenient to start with the following simple model which gives qualitatively correct results at high density. Consider a hydrogenlike ion with nuclear charge Z immersed in a uniform-electron gas of density n_e. Then the electrostatic potential energy seen by the bound electron is

$$V(r) = -\frac{Ze^2}{r} + \frac{Z-1}{2R_0}e^2\left[3 - \left(\frac{r}{R_0}\right)^2\right], \quad r \le R_0 \qquad (1)$$

where R_0 is the radius of a sphere containing enough free electrons (plus the bound electron) to

neutralize the ion:

$$R_0=\left(\frac{Z-1}{\frac{4}{3}\pi n_e}\right)^{1/3}.$$

The first term is the nuclear potential which gives rise to the normal, hydrogenic spectra. The remaining term denoted by ΔV is the potential generated by the surrounding free electrons. This is the source of the line shift. First-order perturbation theory can be used to estimate the change in frequency:

$$\begin{aligned}\Delta\hbar\omega&=\langle 2p|\Delta V|2p\rangle-\langle 1s|\Delta V|1s\rangle\\&\approx -2\times10^{-22}n_e/Z^2\ \text{eV}.\end{aligned}\tag{2}$$

The first term in brackets in Eq. (1) canceled out, since it is a constant and shifts all levels toward the continuum by the same amount. This is just the high-density expression for continuum lowering given by Stewart and Pyatt.[7] The second term does make a contribution, as it depends on r^2 and affects the $2p$ level more than the $1s$ level. As seen, the shift is always to lower frequencies (to the red) in this model, and it is directly proportional to density. The results of a more sophisticated calculation, discussed below, show similar behavior at high density.

This calculation was improved in two ways. First, the free electron distribution was not assumed to be uniform. Each electron is attracted by the nucleus and repelled by other electrons causing density variations. This effect was taken into consideration by solving the nonlinear Poisson equation to find a self-consistent potential and to determine the electron distribution function. Second, perturbation theory was not used to find the shift in frequency. Instead the Schrödinger equation was solved numerically for the energy levels.

Poisson's equation for a hydrogenic ion immersed in a plasma is

$$\frac{1}{r}\frac{d^2}{dr^2}rV=4\pi e^2[n_e(r)+|\psi(r)|^2-n_i(r)],\tag{3}$$

with the boundary conditions

$$V(\infty)=0,$$
$$V(r)=Ze^2/r,\quad r\to 0.$$

Here ψ is the normalized wave function of the bound electron, n_e is the number density of free electrons, and n_i is the number density of neighboring ions. The number densities are given classically by Maxwell-Boltzmann statistics and depend on the potential V:

$$\begin{aligned}n_i(r)&=n_0e^{-V/kT},\\n_e(r)&=n_0\frac{\sqrt{\pi}}{2}\int_{p_0}^{\infty}\exp\left(-\frac{p^2}{2mkT}+\frac{V+V_q}{kT}\right)\\&\quad\times\frac{p^2dp}{(2mkT)^{3/2}},\end{aligned}\tag{4}$$

where $p_0=[2m(V+V_q)]^{1/2}$. This definition for the free electrons is the classical expression used by Stewart and Pyatt and by Rozsnyai, namely, that the kinetic energy is greater than the potential energy. The term V_q contains the quantum-mechanical corrections to the potential and is discussed in Sec. IIB. It was included for completeness but was found to make less than a 1% contribution to the line shift. The effects of Fermi degeneracy were not included because the high-density experiments, to be discussed, will be at a sufficiently high temperature that the amount of degeneracy should be negligible. For convenience, Eq. (4) can be rewritten as

$$n_e(r)=n_0\{2(y/\pi)^{1/2}+[1-\text{erf}(\sqrt{y})]e^y\},\tag{5}$$

where $y=(V+V_q)/kT$.

The bound-state wave function ψ was found by solution of the Schrödinger equation in a potential V' generated by the nucleus, free electrons, and neighboring ions, namely:

$$\frac{1}{r}\frac{d^2}{dr^2}rV'=4\pi e^2[n_e(V)-n_i(V)],\tag{6}$$

with boundary conditions

$$V'(\infty)=0,$$
$$V'(r)=Ze/r,\quad r\to 0.$$

Again n_e and n_i are the number densities of free electrons and neighboring ions, determined in Eq. (3) from the self-consistent potential V. In practice there is not much difference between the potentials V and V' for high-Z hydrogenic ions, as they only differ by the contribution of the one bound electron. The main contribution is from the much larger number of free electrons.

The equation for the bound-state wave functions is

$$-(\hbar^2/2m)\nabla^2\psi_n+V'(r)\psi_n=E_n\psi_n.\tag{7}$$

The bound-electron density used in Eq. (3) is the statistical sum of $1s$ and $2p$ wave functions,

$$|\psi|^2=(|\psi_{1s}|^2+A|\psi_{2p}|^2)/(1+A),$$

where the weight factor A is given by Boltzmann statistics, $A=3\exp(-\hbar\omega/kT)$. Since the equations will be applied to ions with only one bound electron, the Hartree-Fock formalism used by Rozsnyai for a general ion, does not enter here. For

application to materials of higher Z than neon, relativistic corrections should be considered.

Equations (3)–(7) form a set of coupled nonlinear equations which were solved numerically by iteration. The method was to start with Eq. (3) using unperturbed, hydrogenic wave functions. Convergence to 3 digits in the energy eigenvalues occurred after 2–3 iterations. The eigenvalues were then used to calculate the new frequencies for the $2p$-$1s$ transition.

B. Quantum-mechanical considerations

Quantum-mechanical properties of the free electrons enter through the term V_q in Eq. (4). These include, in an approximate way, the wave properties of the electron and the effect of using an antisymmetric wave function. Without the quantum-mechanical corrections ($V_q = 0$), Eq. (5) would give the unphysical result that the electron density becomes infinite at the nucleus. This is corrected by V_q, but the effect is negligible for calculating the line shift. The reason is that the Coulomb potential also goes to infinity at the nucleus, and the infinite electron density produces only a small perturbation around this.

In order to evaluate the full effect of quantum-mechanical corrections, the two most important contributions were used for V_q in Eq. (5), namely, (1) exchange and (2) gradient corrections. It is the second that prevents the electron density from becoming infinite. For a review of the quantum-mechanical corrections, see Refs. 9 and 10.

The exchange term results from antisymmetrizing the electron wave function. Physically, it prevents two electrons from occupying the same place with the same quantum numbers, in accordance with the Pauli exclusion principle. The high-temperature expression for the exchange energy of free electrons is[11]

$$V_{ex} = -(\pi e^4 a_0) n_e / kT .$$

This contribution becomes small at high temperatures because of the large number of quantum states available to the electron.

The correction which constrains the electron density to remain finite is the gradient contribution, as discussed by More[9]:

$$V_{grad} = \frac{\sigma}{4} \frac{\hbar^2}{2m} \left(\frac{\nabla n}{n} \right)^2 .$$

It prevents the formation of a large electron-density gradient. There is some uncertainty in the value of σ; it takes on values between 1 and $\frac{1}{9}$ for different theoretical models. Various values of σ were used by More to calculate the electron density at the nucleus, and he compared the results

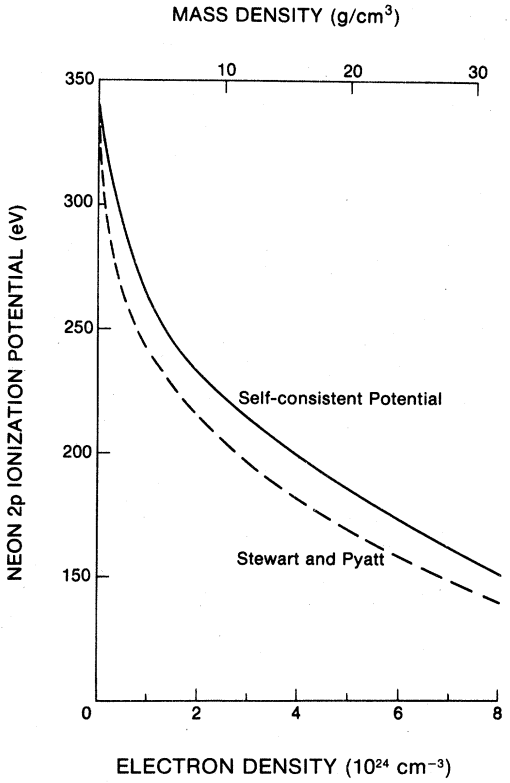

FIG. 1. Ionization potential for the $2p$ energy level in Ne^{+9}.

with a full quantum-mechanical treatment of the free electrons (augmented plane wave). He found that excellent agreement was obtained for $\sigma = 0.483$. This was the value used here.

Another effect that must be considered is the lowering of the continuum. At some density, the $2p$ level will be sufficiently close to the continuum that the oscillator strength for transition will become small. Figure 1 shows how the neon $2p$ ionization potential changes with density at $T = 750$ eV for both the self-consistent calculation and the Stewart and Pyatt high-density model. The ionization potential is about 10% larger than would be obtained from Stewart and Pyatt approximation $[I = I_0 - \frac{3}{2}(Z-1)e^2/R_0]$, mainly due to the second term in brackets in Eq. (1). The fractional oscillator strength defined as

$$\frac{\int \psi_{2p}^2 r^4 dr}{\int (\psi_{2p}^2)_0 r^4 dr}$$

was found to decrease by only 3% at 20 g/cm³. Thus, the neon Lyman-α line should exist at least up to this density.

One source of uncertainty in the model is the boundary condition for the bound electron. If there are other ions of the same kind nearby, there

is a possibility for tunneling and the formation of band structure. This was treated in an approximate way by Rozsnyai.[11] For the present application, this should not be a problem because (1) the ion of interest is only an impurity and the probability is small for finding a neighboring ion of the same ionic species for tunneling. (2) The ion-ion coupling parameter is sufficiently small ($\Gamma < 1$) that the ions are far from being in an ordered lattice. Thus, the usual boundary condition $\psi(\infty) = 0$ was used. Nevertheless, there could still be some distortion in the tail of the wave function, causing the energy levels to broaden. If the result is less than electron impact broadening then it will not affect the conclusions given here. If it is larger, then it will become more difficult to determine the position of the line.

Another source of difficulty could be the presence of free electrons in resonance states that produce line satellites.[12] The shielding due to these states has not been properly included in the model. Further, the presence of satellites might obscure the amount of line shift by overlapping with the line. Such effects were not included here, but could be if experiments show them to be an important factor.

C. Scaling of the line shift with Z

These calculations were done with neon ($Z = 10$) because its line-shift characteristics are well matched to the temperatures and densities anticipated in near-term laser-fusion experiments. To estimate the shift for other materials, it is useful to rewrite the basic equations in terms of dimensionless quantities. Distances will be written in terms of the 1s Bohr orbit radius a_0/Z and energy will be in terms of the 1s binding energy $Z^2e^2/2a_0$.

In these units the Schrödinger equation (7) becomes

$$\frac{1}{x}\frac{d^2}{dx}x\psi(x) + \left(\epsilon_n - v - \frac{l(l+1)}{x^2}\right)\psi(x) = 0\,,$$

where $\psi(x) = (a_0/Z)^{3/2}\psi(r)$, $\epsilon_n = E_n(2a_0/Z^2e^2)$, $v = V(2a_0/Z^2e^2)$, $x = rZ/a_0$, and $\psi(x)$ satisfies the normalization criterion

$$\int |\psi(x)|^2 x^2 dx = 1\,.$$

The Poisson equation (2), becomes

$$\frac{1}{x}\frac{d^2}{dx^2}(xy) = \alpha^2[\bar{n}_e(y)/\bar{n}_0 + e^{-y} + (1/Z)|\psi(x)|^2/\bar{n}_0]\,, \tag{8}$$

where $y = V/kT = v/\tau$, $\tau = kT(2a_0/Z^2e^2)$, $\bar{n} = na_0^3/Z^4$, and $\alpha^2 = 8\pi\bar{n}_0/\tau$. In these units, the boundary conditions are

$$y(x) = 2/x, \quad x \to 0\,,$$
$$y(\infty) = 0\,.$$

All the terms in the above equations are independent of Z, except the contribution of the bound electron in the Poisson equation which varies as $1/Z$. This term becomes insignificant as Z increases; i.e., the self-consistent potential will be mainly determined by the $Z - 1$ free electrons. Also, the quantum-mechanical corrections [not included in Eq. (8)] will be Z dependent. The gradient term will vary as Z^2 and the exchange term Z^4. For $Z = 10$, these were insignificant; for higher Z, they could become important.

Neglecting symmetry breaking by the bound electrons and quantum corrections, the following scaling law is evident: Let $\Delta\hbar\omega_0$ be the line shift for an ion of charge Z_0 in a plasma of temperature T_0 and density n_0. Then the line shift for an ion of charge Z is

$$\Delta\hbar\omega = \Delta\hbar\omega_0(Z/Z_0)^2\,,$$

at a density $n = n_0(Z/Z_0)^4$ and temperature $T = T_0(Z/Z_0)^2$. The accuracy of this scaling law is shown in Fig. 2 which plots the calculated line

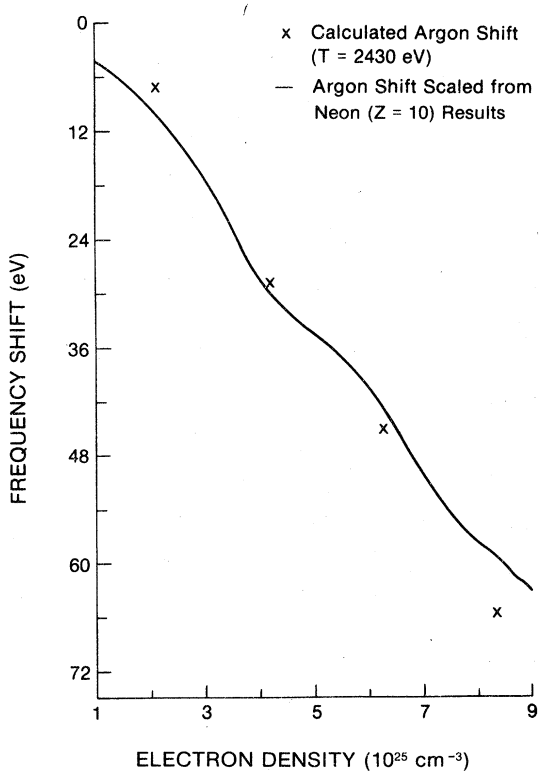

FIG. 2. The calculated frequency shift of argon Lyman α compared with results scaled from neon calculations.

shift for argon ($Z=18$) at $T=2430$ eV compared with the results scale from neon ($Z_0=10$, $T_0=750$ eV). The fractional deviation is on the order of 10%.

III. RESULTS

As an application of the model, the frequency shift of the neon Lyman-α line was calculated for a neon impurity in a deuterium-tritium plasma. Plotted in Fig. 3 is the line shift measured from the unshifted position (1020 eV) as a function of density for $T_e=750$ eV. Also shown, for comparison, are the results from two simpler models: the uniform-electron distribution Eq. (2), and linearized Debye-Hückel theory. The latter gives an energy shift of

$$\Delta E_{\mathrm{DH}} = -\tfrac{1}{2}Ze^2\lambda_D^{-2}\int(\psi_{2p}^2-\psi_{1s}^2)r^4dr$$

$$= -4.8\times10^{-21}n_e/T_{\mathrm{eV}}\ \mathrm{eV},$$

using first-order perturbation theory. For these conditions, the uniform-electron distribution is the better approximation, a result given by Stewart and Pyatt for the region near the nucleus. Both of the simpler models give frequency shifts only to the red. In contrast, the more exact, self-consistent potential can produce a shift in either direction. At low densities, there are sharp oscillations from blue to red of magnitude ~1 eV. Here the line shift is very sensitive to density, and the theory might not be sufficiently accurate to predict the results. Further, at these frequencies the resolution of x-ray spectrometers is about 1 eV so that the line shift cannot be accurately resolved. However, above about 4 g/cm^3 there is a definite shift to lower frequencies that increases almost linearly with density. It is here that comparison between theory and experiment can be made.

There is no *a priori* reason why the line should shift to either the blue or red. At low densities the direction of the shift is very sensitive to the model used; it can change if the bound-state wave function in Eq. (3) is neglected or if first-order perturbation theory is used instead of a full solution of the Schrödinger equation. At higher densities the shift is sufficiently large, that the general trend remains unchanged.

There is a temperature dependence to the line shift which is illustrated in Fig. 4. At the lower temperatures (~500 eV), there can be substantial deviations from the uniform-electron model. There is a 50% difference at 20 g/cm^3. The reason is that the lower temperature electrons are more strongly influenced by the Coulomb potential of the nucleus, whereas at higher temperatures they move more freely and can approximate the uniform-electron model. For temperatures between 750 and 1000 eV the line shift is almost independent of temperature for $\rho>5$ g/cm^3, and it deviates from the uniform-electron model by less than 10%. It is in this high-density, high-temperature region that the line shift could be measured in laser-fusion experiments. One important ques-

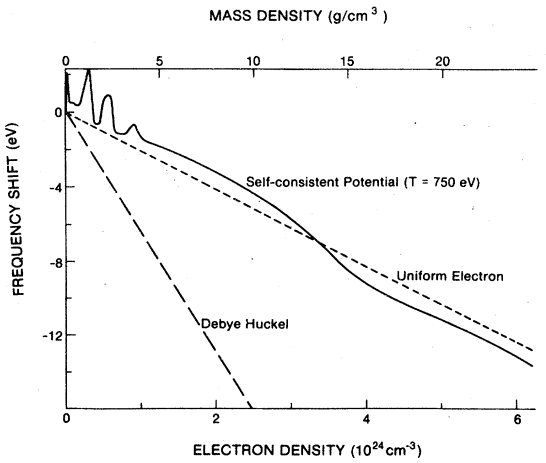

FIG. 3. Neon Lyman-α frequency shift compared with results from the uniform-electron and Debye-Hückel models.

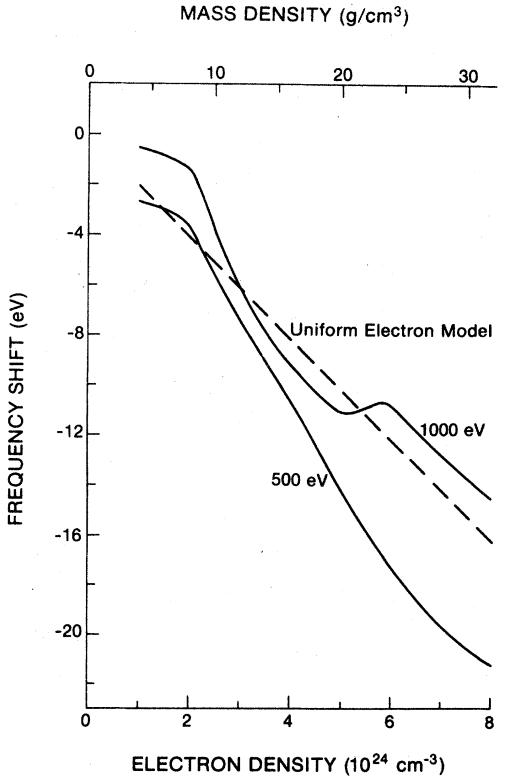

FIG. 4. Temperature dependence of the neon Lyman-α line shift.

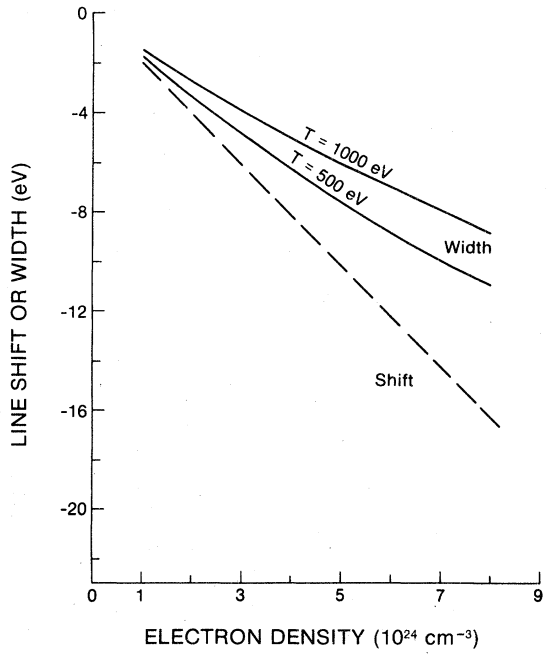

FIG. 5. The shift (uniform-electron model) and width of neon Lyman α.

tion is whether line broadening will obscure the amount of line shift.

For the conditions here, the most important processes for line broadening are (1) opacity, (2) electron impact broadening, and (3) ion-Stark broadening. The first can be eliminated by keeping the neon concentration sufficiently small that the optical depth of the line is less than 1. For the implosion simulation discussed in Sec. IV, the neon Lyman-α line remained optically thin for most of the compression when the neon concentration did not exceed 1% of the total ionic density. Then the dominant broadening mechanism for the peak of the line was electron collisions. Ion-Stark broadening should not affect the peak significantly; it mainly broadens the wings of the line. (Nevertheless, this effect was included in the computer simulation discussed in Sec. IV.) These different broadening mechanisms are discussed in the Appendix.

Figure 5 shows how the line shift compares with the calculated amount of broadening from Eq. (A3). As seen, the shift is greater than the broadening, so that the position of the line should be measurable. However, there are uncertainties in the theory of electron impact broadening, and if the result is substantially larger than estimated here, then the amount of line shift will become difficult to measure.

IV. APPLICATION TO LASER-FUSION EXPERIMENTS

Diagnostics for high-density experiments are of major concern to the laser-fusion community. If the neutron yield always occurred at peak density then there would be no problem; neutron diagnostics such as activation[2] or knock-ons[3] would be adequate. Of course, such neutron timing must occur to obtain energy break-even. However, the immediate goal of near-term experiments is to demonstrate high density rather than yield, and it would be desirable to relax constraints on the timing of neutron production. That would permit the use of targets and laser pulses that are optimized solely for high compression. After compression has been demonstrated, the next step would be to produce high density and high yield simultaneously. Thus, it is valuable to have a diagnostic for high density, independent of neutrons, for near-term experiments. The line shift is such a diagnostic. It depends mainly on density, though the intensity of emission is determined, in part, by electron temperature. The electron temperature is much easier to control than the ion temperature (needed for neutron production), as it is less sensitive to the timing of shocks in the fuel.

However, the line-shift diagnostic will have problems with detection of the signal. There are two sources of difficulty: (1) The line profile will be a superposition of lines emitted from different densities at different times during the implosion. One result is that the intensity from low-density emission can be an order of magnitude larger than the high-density emission and obscure the amount of line shift occurring at peak compression. (2) The second difficulty is that the line-to-continuum ratio can be so small that a clear determination of the shift is impossible. These difficulties can be partly eliminated by using an x-ray streak camera to resolve the temporal emission of the spectral line. This is state of the art technology; the Rutherford Laboratory has had initial success in time resolving a spectral line.[13] From the streak picture, we would see how the line frequency changes during the compression. Good frequency resolution will not be necessary with the streak camera, since we are not interested so much in the shape of the line, but mainly in its position. However, temporal resolution is not sufficient. The target must be constructed mainly from low-Z material ($\bar{Z} < \sim 6$), otherwise continuum radiation and line attenuation will reduce the line-continuum ratio to the level of noise. Even a 0.5-μm-thick glass shell within the target is sufficient to obscure the line in high-density compressions. For that reason, a plastic microballoon was used in the example below.

To estimate the spectrum that might be seen in the laboratory, the line emission was calculated from the computer simulation of a laser-fusion experiment. The simulation was done with the one-dimensional Lagrangian code LILAC developed at the University of Rochester to study the dynamics of laser-imploded targets. This is a two-fluid code (electrons and ions) that includes hydrodynamic motion together with energy transport from thermal conductivity, shocks, suprathermal electrons, and radiation. Suprathermal electrons from the laser-target interaction were transported with 20 energy groups. Radiation was transported in 50 frequency groups using opacity tables[14] developed at Los Alamos. The Thomas-Fermi equation of state was used throughout.

The spectral line profile was calculated with the following approximations: (1) The line shift and splitting of the $2p$ and $2s$ energy levels were evaluated with the uniform-electron model (Sec. II). (2) The line shape included electron impact broadening and ion-Stark broadening in the nearest-neighbor approximation, as discussed in the Appendix. (3) Line properties were calculated using the average density and temperature in the fuel. (4) The level populations (which determine the line intensity and optical depth) were determined using the Saha equation to relate $n=2$ to the next stage of ionization and by balancing radiation and collision rates for the ratio of $n=2$ to 1. It is felt that these approximations preserve the essential features on the line shift. However, when the experiments are done, it might be desirable to improve the level of approximation in the modeling.

The computer simulation is for a thick, spherical-shell target that absorbs 0.5-terrawatt (TW) laser power in a 50-psec Gaussian pulse. Such a power level is readily available (or shortly will be) at the major laser-fusion laboratories. It represents power deposited in the target which is not lost to "fast ions" and corresponds to about 2.5-TW incident. A "pie-shaped" diagram of the target is shown in Fig. 6. It is a 20-μm-thick plastic microballoon of inner radius 40 μm, filled with 10-atm DT, 0.5-atm argon, and 0.1-atm neon for the line-shift diagnostic. There is a 50-Å layer of aluminum, deposited on the inner surface of the plastic shell, to improve the implosion dynamics and to provide additional information about density through spectral line emission.

This target is an example of radiationally cooled targets being considered by the University of Rochester (Laboratory for Laser Energetics) for high-density experiments.[15] Radiation from high-Z material (in this case argon) keeps the target sufficiently cool that a high-density compression should be possible. Although neutrons are produced, they occur so far before peak compression (10% peak density) that they are useless here as a high-density diagnostic. Such targets are designed to demonstrate high density in the laboratory rather than neutron yield, and the amounts of argon, DT, and wall thickness are adjusted mainly to produce the desired electron temperature and compression in the fill. The neutron yield is of secondary importance.

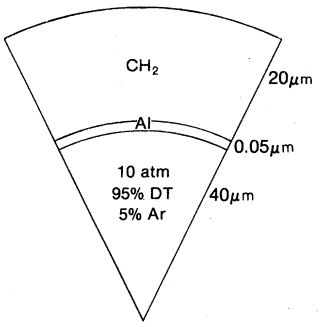

FIG. 6. Target used for the laser-compression simulation.

The time evolution of the average density and temperature in the fuel is shown in Fig. 7. Initially the fuel is shock heated to 1 keV from explosion of the plastic shell, at a density far from peak compression ($\rho \sim 2$ g/cm^3). At this point neutron emission occurs. The fuel then cools by radiation emission and reaches a peak density of 20 g/cm^3 at 600 eV. The neon line radiation is a maximum approaching peak compression, but it is quickly quenched afterward due to cooling in the target.

The high line emission near peak compression suggests that the time-integrated spectrum should easily give information about the maximum density. This does not occur for two reasons. First,

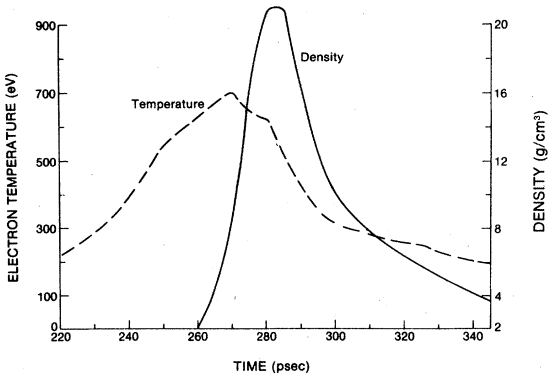

FIG. 7. Average temperature, density in the fuel as a function of time.

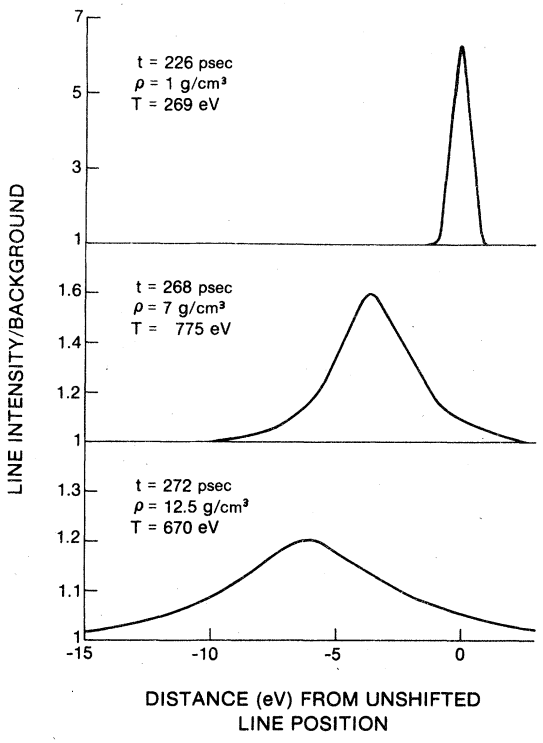

FIG. 8. Line profiles for neon Lyman α emitted at different times during the implosion. Intensity is relative to the background for each time.

high-density broadening of the line reduces its intensity (energy per unit frequency) sufficiently that the total spectrum is completely dominated by the low-density narrow-line emission. Second, the optical depth in the plastic and aluminum shells is highest at peak compression and causes a 50% attenuation of the line. The net result is a sharp spike at the normal position of the line from low-density emission with intensity roughly equal to the background. There is a shoulder from high-density emission, at lower frequency, but it is only 1% of the background and would not be detected.

Some of the difficulty is removed by time resolving the line emission with an x-ray streak camera. This separates the high-density emission from the high-intensity radiation at low density. This is shown in Fig. 8 where the line intensity (relative to the continuum intensity) is plotted for three times during the compression. The early time emission serves as a marker for the normal position of the line. Then the frequency shift can be followed with time until 272 psec when the shift is −6 eV, corresponding to 12 g/cm^3. Afterwards the line is lost in the background, due to attenuation in the shell and low temperature in the target.

This example is not necessarily the optimum for 0.5 TW absorbed. It was chosen just to illustrate a class of simple targets that can demonstrate the feasibility of high-density compressions in the laboratory, but would be difficult to diagnose by any means other than the line shift. Neutrons are produced too far before peak compression to be useful, and the temperature at peak compression is too low to use argon line broadening. One other possible diagnostic is the relative intensity of neon satellite lines.[12] It still remains to determine if satellite lines will overlap the shifted Lyman-α line and distort the line position, or whether they will be simultaneously shifted. For this target, there should not be any other lines that could distort the spectrum.

V. SUMMARY

The frequency shift of the Lyman-α spectral line in neon is found to be a good measure of density in the region anticipated for high-compression laser-fusion experiments. This diagnostic could be especially valuable for near-term experiments if there is difficulty producing neutrons close to peak compression so that they become useless for estimating peak density. Calculation of the spectral line involved solution of the Schrödinger equation in a self-consistent potential determined by the nucleus and the distribution of free electrons and neighboring ions. It is felt that the major physical effects were included in the calculation with the possible exception of resonances, producing line satellites. The results showed that the line shift oscillates from red to blue at low density, but above a density of 4 g/cm^3 (for neon) there is a continuous shift to the red which increases almost linearly with density. In this region the shift could be used to diagnose density.

These calculations were done for a static distribution of electrons with the assumption that fluctuations around the mean would only broaden the line but not significantly change its position. Examination of this assumption requires calculation of the static and dynamic interactions simultaneously as was done by Lee.[16] However, Lee used linear-response theory to describe shielding of the nucleus. In the static limit, this is roughly equivalent to linearized Debye-Hückel shielding, which is not appropriate to high densities as discussed in Sec. III. A more exact treatment is required.

Computer simulations of possible laser-compression experiments show that early emission of the line at low densities produces a reference point from which to measure the amount of line shift. However, there might be difficulty extracting information from the time-integrated line profile as emission early in time could obscure the emis-

sion from peak compression. This is overcome if the spectrum can be time resolved using an x-ray streak camera. In addition, only low-Z target material ($\bar{Z} < \sim 6$) can be used, to prevent a high background and line attenuation.

The theory of x-ray line shifts still has not been tested in the laboratory. Near-term laser-fusion experiments should provide the means for examining this and other properties of ions in a high-density plasma.

ACKNOWLEDGMENT

This work was partially supported by the following sponsors: Exxon Research and Engineering Company, General Electric Company, Northeast Utilities, Empire State Electric Energy Research Corportation, and New York State Energy Research and Development Administration.

APPENDIX

This section describes the calculation of the intrinsic line profiles used for the computer simulation of the neon Lyman-α frequency shift. One important aspect in determining the line shape is breaking of the Coulomb degeneracy due to free electrons shielding the nucleus. This causes a splitting of the $2p$ and $2s$ energy levels and determines whether the ion-Stark shift will be linear or quadratic. It further introduces an asymmetry into the line profile.

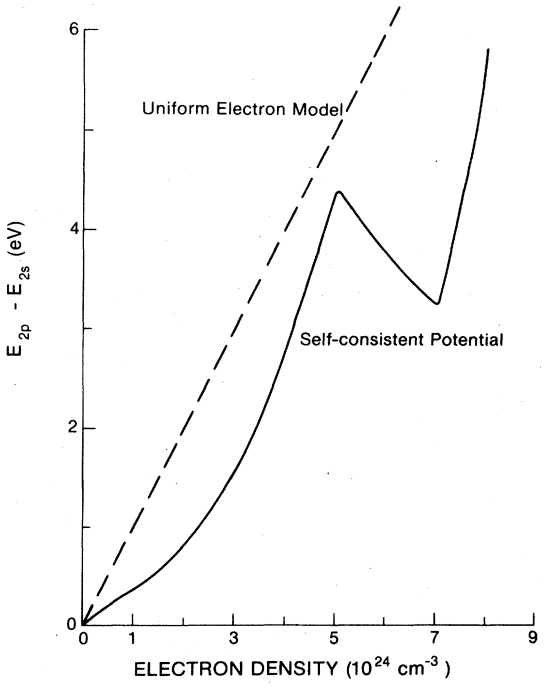

FIG. 9. Breaking of the $2p$, $2s$ Coulomb degeneracy as a function of density in neon.

Figure 9 shows how the $2p$ and $2s$ energy levels diverge as a function of density for the self-consistent potential (Sec. II) for neon. An estimate for the amount of splitting can be obtained from the uniform-electron model (Sec. II) using first-order perturbation theory:

$$E_{2p} - E_{2s} = 1 \times 10^{-22} n_e / Z^2 \text{ eV}.$$

At an electron density of 5×10^{24} cm^{-3} (20 g/cm^3), the splitting is 5 eV and has a substantial effect on the ion-Stark broadening. In comparison, the fine structure splitting for neon is only 0.2 eV and can be neglected. (At this density the electron impact broadening is about 5 eV.)

The ion-Stark effect occurs when electric fields from neighboring ions perturb the orbits of bound electrons. Let $V(\vec{R}+\vec{r})$ be the potential energy between the bound electron and neighboring ions, where $\vec{r}$ gives the position of the bound electron, and $\vec{R}$ gives the position of the neighbor, relative to the nucleus. Then, in the dipole approximation, the perturbation is $U = r(\partial V/\partial r)_R Y_{10}(\hat{r})$ with the z axis along the gradient of V. This term will shift (and mix) the $|n=2, l=1, m=0\rangle$ and $|2,0,0\rangle$ states, leaving both $|2,1,1\rangle$ and $|2,1,-1\rangle$ unchanged. Writing the new eigenfunctions as

$$|1\rangle = a|2,1,0\rangle + b|2,0,0\rangle,$$

$$|2\rangle = b|2,1,0\rangle - a|2,0,0\rangle,$$

with $a^2 + b^2 = 1$, the wave-function coefficients and eigenvalues are determined by the matrix equation:

$$\begin{pmatrix} E_{2s} - E & U \\ U & E_{2p} - E \end{pmatrix} \begin{pmatrix} a \\ b \end{pmatrix} = 0 .$$

This has the solutions

$$E_{1,2} = \{(E_{2s} + E_{2p}) \pm [(E_{2p} - E_{2s})^2 + 4U^2]^{1/2}\}/2 ,$$

with

$$a = U/[U^2 + (E_1 - E_{2s})^2]^{1/2} ,$$

$$b = (E_2 - E_{2p})/[U^2 + (E_2 - E_{2p})^2]^{1/2} .$$

The + or − sign is chosen so that $E_1 \to E_{2s}$ and $E_2 \to E_{2p}$ as $U \to 0$ with $E_{2p} > E_{2s}$. When the levels are degenerate ($E_{2s} = E_{2p}$) then the states are shifted in opposite directions with equal probability and with magnitude U, i.e., the linear Stark effect. When the Coulomb degeneracy is broken ($E_{2s} \neq E_{2p}$) then the states are equally shifted around the mean $(E_{2s} + E_{2p})/2$ but with different weights. Finally, in the limit when U is much smaller than the level spacing, the $2p$ and $2s$ states become decoupled and $|2,1,0\rangle$ is shifted by $U^2/(E_{2s} - E_{2p})$

(i.e., quadratic Stark effect). Thus, the amount of degeneracy breaking will play an important role in determining the shape of the Stark broadened profile. The average value of U can be estimated for a neighboring hydrogen ion as $U \sim r_{2p} e^2/R_0^2$, where R_0 is the ion-sphere radius and r_{2p} is the radius of the $2p$ orbit ($r_{2p} = 2.5 \times 10^{-9}$ cm for neon). At an electron density of 5×10^{24} cm^{-3}, R_0 is 8×10^{-9} cm which gives $U = 6$ eV. This is comparable to the splitting of the $2p$ and $2s$ energy levels, and shows that breaking of the Coulomb degeneracy must be included for the line-profile calculation.

The actual values of U were calculated from the nearest-neighbor approximation which gives good agreement with more detailed calculations,[17] at high density. This model assumes that the major contribution to ion Stark broadening comes from the closest, neighboring ion. Let $n_i(r)$ be the distribution function for neighboring ions and $W(r)dr$ the probability that the nearest ion is at a radius r. Then W satisfies the equation

$$W(R)dR = \left(1 - \int_0^R W(r)dr\right) n_i(R) 4\pi R^2 dR ,$$

where the term in parantheses gives the probability of not finding the nearest neighbor at radii smaller than r. This equation has the solution:

$$W(R) = AR^2 \exp\left(-\int_0^R n_i(r) 4\pi r^2 dr\right),$$

where A is determined from the normalization condition $\int_0^\infty W(r)dr = 1$. The energy change caused by an ion at R is

$$E(R) = \langle 2p | r | 2p \rangle V'(R) = (5a_0/Z) V'(R) .$$

The probability that the energy level will be shifted by E is

$$P(E)dE = W(R)dR .$$

Hence the intrinsic line profile due to ion-Stark broadening is

$$P(E) = W(R)/[(5a_0/Z) V''(R)] .$$

For these calculations, a Debye-Hückel potential was used to estimate $V(R)$.

This profile must be further convoluted with a Lorentzian profile for electron broadening, which will also broaden the unshifted $2p$ component. The expression for the half width was taken from Griem[18]:

$$\Gamma = 3 \times 10^{-22} (2.4 - \ln y) n_e/(Z^2 \sqrt{T}) , \tag{A1}$$

where

$$y = 4 \times 10^{-22} n_e (Z^2 T) . \tag{A2}$$

The total line profile is

$$L(E) = \frac{1}{\pi} \int P(E') \frac{\Gamma dE'}{\Gamma^2 + (E - E')^2} . \tag{A3}$$

The expressions in this section for ion broadening were developed for the dipole approximation. For the actual calculation of profiles, quadrupole corrections, and fine-structure splitting were included.

[1]For example: B. Yaakobi, D. Steel, E. Thorsos, A. Hauer, B. Perry, S. Skupsky, J. Geiger, C. M. Lee, S. Letzring, J. Rizzo, T. Mukaiyama, E. Lazarus, G. Halpern, H. Deckman, J. Delettrez, J. Soures, and R. McCrory, Phys. Rev. A 19, 1247 (1979).

[2]F. Mayer and U. Reasel, J. Appl. Phys. 47, 1491 (1976); E. M. Campbell, H. G. Hicks, W. C. Mead, S. S. Glaros, L. W. Coleman, and W. B. Laird, Report No. UCRL-79778, 1977 (unpublished).

[3]S. Skupsky and S. Kacenjar (unpublished).

[4]H. F. Berg, A. W. Ali, R. Lincke, and H. R. Griem, Phys. Rev. 125, 199 (1962); J. G. Greig, H. R. Griem, L. A. Jones, and T. Oda, Phys. Rev. Lett. 24, 3 (1970); H. R. Griem, *Spectral Line Broadening by Plasmas* (Academic, New York, 1974), pp. 146–153.

[5]J. C. Weisheit and B. F. Rozsnyai, J. Phys. B 9, L63 (1976).

[6]B. F. Rozsnyai, J. Quant. Spectrosc. Radiat. Transfer 15, 695 (1975).

[7]J. C. Stewart and K. D. Pyatt, Astrophys. J. 144, 1203 (1966).

[8]R. D. Cowen and J. G. Kirkwood, J. Chem. Phys. 29, 264 (1958).

[9]R. More, Phys. Rev. A 19, 1234 (1979).

[10]S. G. Brush, in Progress in *High Temperature Physics and Chemistry*, edited by C. A. Rouse (Pergamon, Oxford, 1967).

[11]B. F. Rozsnyai, Phys. Rev. A 5, 1137 (1972).

[12]J. F. Seely, Phys. Rev. Lett. 42, 1606 (1979).

[13]Rutherford Laboratory annual report, 1978, p. 453, (unpublished).

[14]W. F. Huebner, A. L. Merts, N. H. Magee, and M. F. Argo, Report No. LA-6760, 1977 (unpublished).

[15]S. Skupsky and R. L. McCrory, Bull. Am. Phys. Soc. 24, 945 (1979); R. L. McCrory, S. Skupsky, J. Delettrez, and R. S. Craxton, Proceedings of the 12th European Conference on Laser Interaction with Matter, Moscow, USSR, 1978 (unpublished).

[16]R. W. Lee, J. Phys. B 12, 1129 (1979.

[17]C. F. Hooper, Phys. Rev. 165, 215 (1968).

[18]H. R. Griem, Phys. Rev. A 17, 214 (1978).